Effect of Serum Components on Styrene/Butyl Acrylate Latex Film Formation: An In Situ Examination by Ultramicroscopy

Amauri José Keslarek, Fernando Galembeck

Instituto de Química, Universidade Estadual de Campinas 13083-970, Campinas SP, Brasil

Received 18 October 2001; accepted 11 March 2002

ABSTRACT: Film formation by a surfactant-stabilized, peroxide-initiated styrene/butyl acrylate latex was followed in situ by ultramicroscopy. The effects of latex serum components on film formation were observed first by the subjection of the latex to extensive dialysis and then by the separate addition of salt and surfactants. Domains of different particle concentrations were observed in the latex dispersion during liquid evaporation, and their positions were related to those of defects in the dry film. Films obtained with the dialyzed latex showed macroscopic defects, which were not seen in the as-prepared latex. Partially reconstituted latex (dialyzed, with the later addition of salt but not surfactant) behaved like the as-prepared latex. © 2002 Wiley Periodicals, Inc. J Appl Polym Sci 87: 159–167, 2003

Key words: films; surfaces; surfactants

INTRODUCTION

Latex film formation has been examined in great detail since the early 1950s,[1–4] and the large body of results in the literature has been reviewed;[5–8] this has created a good understanding of the problem, but there are some conflicting views. The driving forces for the morphological transformations of particles into a film, during and after water evaporation, are capillary forces, polymer/water interfacial tension, polymer surface tension, and the other forces due to the residual water left among the particles.

Latex film formation is also a topic of great practical interest[9] that has attracted the attention of many researchers interested in paints, coatings, and adhesives, as well as the fabrication of products such as gloves and condoms.

There is still some variability in the meaning of the words *film* and *coalescence*, and in this work, we use these terms following Joanicot et al.,[10] who considered coalescence to be the fusion of particles with the expulsion of the surface-active species used to stabilize the dispersion.

For paints, the leveling or roughness of the dry surface is a matter of great importance because it will determine its optical and cleaning characteristics.[11] Surface tension[12] is a powerful driving force toward the formation of a flat, smooth surface, but its action is retarded or severely restricted by many factors, such as the presence of particulate pigments, tiny bubbles, and poor adhesion and coalescence of latex particles, as well as low particle plasticity.[13,14] The copolymer nature of many types of latexes adds the possibility of variability in the composition of the film surface,[15] allowing for the consequences of the Marangoni effect,[16] which causes mechanical stresses and consequent film deformation.

The direct observation of latex drying and film formation in real time is desirable, as it can reveal information about the dynamics of the particles and their aggregation, clustering, and morphological changes. However, because of the small particle sizes and the presence of water and other volatile materials, the use of the more common types of light and electron microscopy is not possible in this context. Newer techniques, such as small-angle X-ray scattering (SAXS), environmental scanning electron microscopy (ESEM), and confocal microscopy have already been used,[17–19] and they have contributed new information. For instance, Dingenouts and Ballauff[17] used SAXS and reported that when polystyrene (PS) or poly(methyl methacrylate) (PMMA) latexes were dried below the polymer glass-transition temperature (T_g), particle deformation did not occur from the dilute suspension to a closely packed sphere system, and a long-range order was not achieved during the drying process. He and Donald[18] observed, by using ESEM, that a PMMA latex formed ordered particle arrays in the absence of salt, but salt addition led to the formation of disordered flocs. Ito et al.[19] determined the anionic PS particle concentration as a function of the height above

This article is a contribution from the Millennium Institute or Complex Materials/MCT.

Correspondence to: F. Galembeck (fernagal@iqm.unicamp.br).

Contract grant sponsor: Fapesp.
Contract grant sponsor: Pronex/Finep.
Contract grant sponsor: CNPq.

a glass substrate, and they found greater particle distribution uniformity at higher ionic strengths, using confocal microscopy, thereby supporting a wall effect on the particle dispersion.

Ultramicroscopy is another interesting possibility for the observation of latex film formation, and it has not been previously used. This is an old technique[20] but currently a powerful and practical one because of the availability of diode lasers and video microscopy equipment, along with the associated facilities for image processing. The sample is observed in an optical microscope dark field while a laser beam illuminates it at 90° to the axis of the objective. The scattered light is captured through the objective with a video camera, and the image is recorded with a videocassette. Ultramicroscopy can be used to observe particles much smaller than the wavelength of light if these scatter strongly enough to be observed as bright spots in a dark field.[21] It does not give direct morphological information on individual particles, but it allows the observation of particle motion and clustering. Motion is observed by the displacement of the bright spots in the x–y plane or by spot defocusing due to motion in the z axis. Clustering is seen as the concerted motion of neighboring spots. Particle coalescence can also be observed indirectly by the monitoring of the disappearance of scattering bright spots; aggregated but uncoalesced particles are easily observed as clusters of bright spots in the dry film. Because the image contrast is dependent on the scattering ability of the different sample domains, this technique is also excellent for detecting sharp refractive-index gradients, throughout the dry film, arising from open and closed pores and from polymer chemical composition gradients. Yoshida et al.[22] used ultramicroscopy associated with confocal microscopy to observe ordered–disordered colloidal phase transitions.

In this work, we examined the effect of latex serum components on film formation with a low-T_g styrene/butyl acrylate latex often used in paint making. For this purpose, we performed experiments with the following samples: (1) the as-prepared latex; (2) the same latex, but after dialysis for the removal of micromolecular and ionic species; and (3) the dialyzed latex after salt or surfactant addition, as required for the evaluation of the effect of serum components.

EXPERIMENTAL

The latex was prepared by emulsion polymerization in a covered, 1-L kettle glass reactor in which were fitted a two-wing turbine-type stirrer, a thermometer, a condenser, a burette for the initiator addition, and a separation funnel for the controlled addition of the emulsion containing monomers, water, and surfactant. The reactor was immersed in a thermostatic water bath.

The reagents used were MilliQ deionized water, ammonium hydroxide, styrene, acrylic acid, butyl acrylate and sodium formaldehydesulfoxylate (Basf), ammonium persulfate (Peroxyde Chimie), Rhodacal DSB (disodium dodecyl diphenylether disulfonate, 45% aqueous solution, Rhodia), and *t*-butyl hydroperoxide (Akzo). Renex 300 (ethoxylated nonylphenol 30 EO, Oxiteno) was used for postaddition on the dispersion. Before use, styrene was distilled under N_2 at a reduced pressure.

The monomer emulsion was prepared in a beaker by the dissolution of 8.8 g of surfactant in 88.8 g of water followed by monomer addition (88.6 g of styrene, 102.0 g of butyl acrylate, and 3.81 g of acrylic acid) and stirring. Water (76.4 g) was added to the reactor, and this was purged with N_2, stirred at 300–350 rpm, and heated at 75°C, at which point surfactant (2.23 g) was added, followed by 0.27 g of ammonium persulfate. An ammonium persulfate solution was separately prepared (1.38 g at 0.22 mol L^{-1}) for feeding during polymerization. The monomer emulsion and the ammonium persulfate solution were added simultaneously to the reactor, at 4 h and 4.5 h, respectively. The temperature was kept at 80 $\pm$ 1° C during the first 3 h and then was increased to 85°C. After the reagent addition was complete, 10% solutions of 1 g of *t*-butyl hydroperoxide and 1 g of sodium formaldehydesulfoxylate were added simultaneously for 30 min to eliminate the residual monomer.

The final dispersion was cooled to room temperature and filtered through a 200-mesh screen, at which point 1.1 g of coagula was collected, and its pH was adjusted to 7.5 with 12.5 mL of 15% ammonium hydroxide; it yielded 402 mL of a dispersion containing 46.6 wt % solids. This is called the *as-prepared latex* in forthcoming sections. An aliquot of the latex was extensively dialyzed through a regenerated cellulose membrane until the conductivity of the external water was less than 2 μS. The conductivity of the as-prepared dispersion was 8.3 mS, and that of the dialyzed latex was 0.80 mS.

In the film formation experiments, five samples were used: (1) as-prepared latex (AP), (2) dialyzed latex (DL), (3) partially reconstituted latex (dialyzed latex after the addition of a 0.4 mol L^{-1} solution of NaCl until it had the same conductivity as the as-prepared latex dispersion; RL1), (4) RL1 latex after 0.9 wt % Rhodacal DSB addition (based on monomers; RL2), and (5) dialyzed latex to which 0.4 wt % Renex 300 (based on monomers) was added (RL3). The final ionic strength of the RL1 dispersion was 0.12 mol L^{-1}, and this dispersion was stable.

For the observation of latex drying and film formation, 0.03–0.04 g of latex was spread on a 1.5 cm $\times$ 1.5 cm glass slide cover kept in a horizontal position on top of a glass slide; this provided a 150-μm initial thickness and 50–70-μm final thickness (of the dry films) when the surface was observed under a micro-

scope within a room with the temperature (18–20°C) and humidity (40–60% relative humidity) controlled. The slide covers were previously washed with ethanol and dried under air. The dispersion surface temperature was monitored with a Minolta/Land Cyclops Compac 3 infrared thermometer. This instrument was a remote temperature meter, allowing real-time measurements of the undisturbed samples.

Film formation experiments were repeated at least three times, and the patterns observed during latex drying and in the dry films were highly reproducible.

Optical microscopy and ultramicroscopy

A Bausch & Lomb microscope was used, coupled to a Sony SSC-C350 camera, a Sony PVM-1350 monitor, and a JVC HR-S7200U videocassette recorder. Reflected light and scattered light (in the ultramicroscopy mode) were used for image formation, with a fiber optical illuminator (Cole–Parmer model 9745-00) and a 3-mW, 670-nm diode laser from RS Components, respectively. Video-recorded images were grabbed and processed with Image-Pro Plus 4.0 software.

Infrared spectroscopy

A Nicolet 520 spectrometer was used. The dispersion samples were previously dried under reduced pressure for 1 h. They were then dissolved in $CHCl_3$, and the solutions were spread on a NaCl crystal surface on which they were dried at first under air and later under reduced pressure for 1 h.

Photoelectron correlation spectrometry (PCS) and ζ potential

A ZetaPlus (Brookhaven) analyzer was used. The effective particle diameter was averaged from 5 runs, and the ζ potential was averaged from 10 individual runs. Measurements were made on 10 μL of latex diluted in 3 mL of a 10^{-3} M KCl solution.

Atomic force scanning probe microscopy

Film-coated slide covers were glued to the sample holder, which was mounted on a Topometrix Discoverer TMX-2010 microscope in which noncontact atomic force microscopy (AFM) images were obtained. Image processing was done with the Topometrix software.

RESULTS

The as-prepared latex contained 46.6 wt % solids, as determined by gravimetry. The effective particle diameters of the AP and DL were 121 and 132 nm, respectively (as determined by PCS), and the ζ potential of the dialyzed latex was −66 'mV. The RL1 latex, to which salt was added after dialysis, presented an effective particle diameter equal to 126 nm, which means that no aggregation occurred because of salt addition, but the dialyzed latex particles may be more swollen than those in the presence of salt.

The events observed during film drying may be arranged into three stages, which are described later and summarized in Table I. A schematic representation is given in Figure 1, in which the film in stages 1 and 2 is depicted as seen under scattered light and stage 3 is represented as seen under reflected light. Film surface temperature changes determined with the infrared thermometer were less than 0.3°C.

AP

In the first minutes after spreading, this latex dries, forming an outer square frame of a transparent polymer film, surrounding a roughly circular liquid layer. Intense motion is observed in this liquid, as represented in Figure 2, showing three consecutive frames, recorded at 30 frames per second, from the same area. Each bright spot corresponds to a particle, and this figure shows that particles enter or leave a pixel in less than 1/30 s. Around 10 min, differentiated domains are observed: strongly scattering (concentrated) and low scattering (dilute) domains are seen, as presented in the schematic drawing in Figure 1 and in the micrograph in Figure 3 (top). The shape of the concentrated domain (cloudy; see Fig. 1, stage 1) is repeated as a dark area in a later drying stage (stage 2) and as a defect in the dry film (stage 3), and this shows that film roughness is associated with the formation of differentiated liquid domains in the latex. Figure 4 is an AFM image from the center of the dry film; it is possible to observe film depressions in close proximity to elevations, reaching heights greater than the particle diameter.

To verify the reason for the differences in the scattering intensities between neighboring domains in the dispersion, we ran further film formation experiments to allow for the collection of aliquots of the two types of domains in stage 1 (high and low light scattering) with a micropipette, and the latex from separate domains was analyzed by Fourier transform infrared (FTIR) spectroscopy, ζ potential, and particle size distribution. The results are as follows. First, the styrene/acrylate ratio in the strongly scattering domains is larger than that in their low scattering neighbors, as demonstrated by the A_{1740}/A_{700} (cm^{-1}) absorbance ratio in the FTIR spectra. The 1740-cm^{-1} band is assigned to C═O, the 700-cm^{-1} band is assigned to the aromatic ring, and the absorbance ratios obtained are 1.67 and 1.89 in the strongly scattering and low scattering domains, respectively. Second, the particle size effective diameters were basically the same in the two domains: 120.5 ± 0.4 nm in the strongly scattering

TABLE I
Features of the Drying Latexes

	AP	DL	RL1
Stage 1	Observed at about 15 min	Observed at about 5 min	Observed at about 30 min
	Concentric drying	Concentric drying	Concentric drying
	Visible structure of high particle concentration	Ring formed, with high scattering ability and contiguous to a dark inner ring	Parallel stripes
	Particle velocity decrease in the inner part of the drying film		Sharp border between dispersion and dry film
Stage 2	Observed at about 35 min	Observed at about 10 min	Observed at about 40 min
	Particles moved independently and faster in the domains with a high scattering light	Ring broadened, particles lost individual motion, intense coalescence at the liquid surface	Radial structures
	Collective particle motion in the central area	Collective particle motion predominated	The central region did not present orderly patterns
Stage 3 (dry film)	Reached at about 45 min	Reached at about 40 min	Reached at about 65 min
	Depressions around the previously high concentration domain	Regular, flat central circle	Film periphery was brighter and smoother
	Bright film, few defects	Depressions throughout the film, low brightness	Noncoalesced particles, both in the central region and in the radial structures

domain and 120.1 ± 0.7 in the low scattering domain. However, observing the particle size distribution histograms, which were obtained with the nonnegatively constrained least-squares algorithm,[23] we find that the particles from the strongly scattering domain show a larger polydispersity than the others, covering the 56–237-nm and 117–121-nm ranges, respectively. Third, ζ potentials are -67 ± 4 mV for the particles in the strongly scattering domain and -58 ± 3 mV in the peripheral region. Consequently, particles of different natures and properties, but the same average size, form the two types of domains.

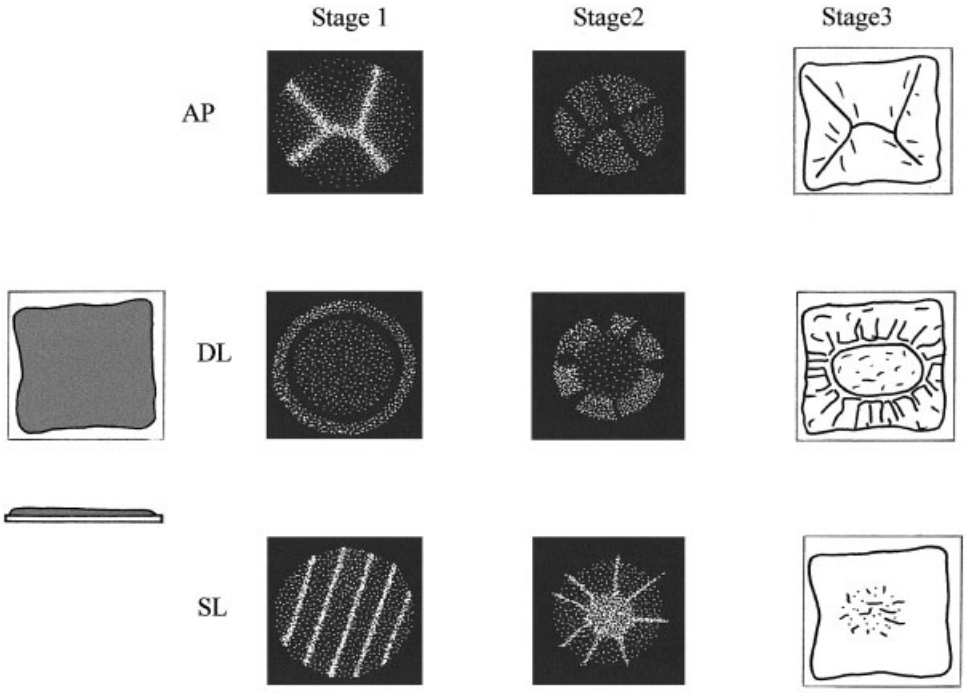

Figure 1 Schematic drawings of AP, DL, and RL1 latex films during stages 1, 2, and 3 of the drying process. The first two stages are represented by dark-field ultramicroscopy drawings, and the third is represented by views of the dry film under reflected light. The drawings in the left column are top and side views of the slide cover with latex soon after spreading.

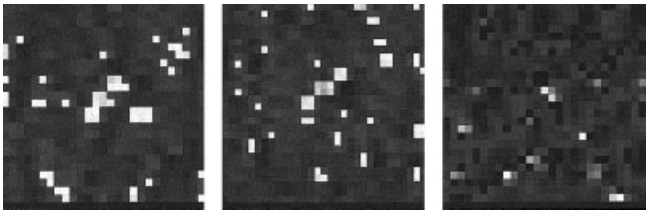

Figure 2 Sequence of three magnified images, from the same film area, taken during AP latex drying (stage 1). The bright pixels correspond to particles in the focusing range. The time difference between consecutive images is 1/30 s. The boxes are 210 μm $\times$ 210 μm.

Around 30 min, the speed of the particles in the (initially) strongly scattering domain is much higher than in the other parts of the film, but the intensity of the scattered light decreases gradually until this domain becomes dark (under 90° illumination), evidencing particle coalescence.

A thin surface polymer film is observed in the final drying stages under reflected light (ca. 40 min) when collective particle or floc motion is observed. The separate particle flocs stop moving at different times, independently of one another.

DL

This latex also forms a central circular liquid region after a few minutes, just like the AP latex. However, this is made out of concentric domains as follows: an outer ring that broadens with time, with slowly moving particles; a second ring with a low scattering ability; and a core with fast moving particles (Fig. 5, top). Other authors[24,25] have also observed outer rings, and they associated them with a high density of flocculated particles. They supported this by rinsing the drying films with water: only the unflocculated particles were dragged. However, we did not find reports on the existence of an inner ring with a low particle concentration in the other systems described in the literature.

Around 10 min (stage 2), a thin polymer film is already observed at the dispersion surface when this is examined under reflected light (Fig. 5, center), and this film covers the fast moving particles in the subsurface liquid film: the motion of the uncoalesced particles is better seen with laser illumination (Fig. 5, bottom), as well as the coalesced structures, which are seen as dark, nonscattering areas. At this time, the ring structure previously described is no longer seen (Figs. 1 and 5, bottom), and the film center dries faster. This causes a large defect in the dry film: a ring-shaped depression surrounding a central region (stage 3, Fig. 1). In this latex, individual particle motion disappears around 17 min, at which point the particles display only collective motion. The drying of both AP and DL samples proceeds by the advancement of a drying front. However, the latter gives films of a lower uni-

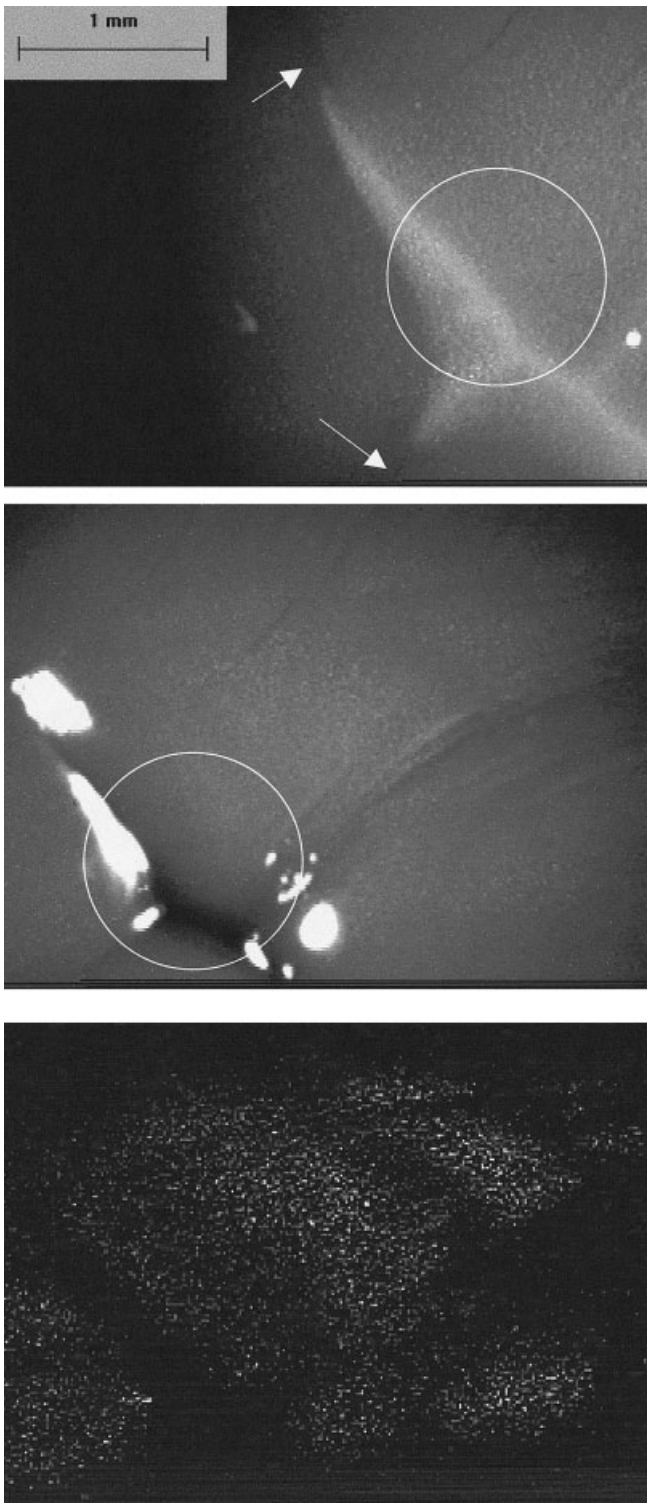

Figure 3 Images from AP latex film formation. The top image was taken during stage 1 under simultaneous reflected light and 90° laser illumination. The arrows show the position of depressions formed later in the dry film. The center image was taken later when the depression formation had progressed, forming strongly reflective domains. The circles in the top and center images indicate the same region. The bottom image is an ultramicrograph taken from the same area as the center image and at the same time, showing domains with different concentrations of scattering particles. In some domains, the particle motion was in concert, and in others, the particles moved independently.

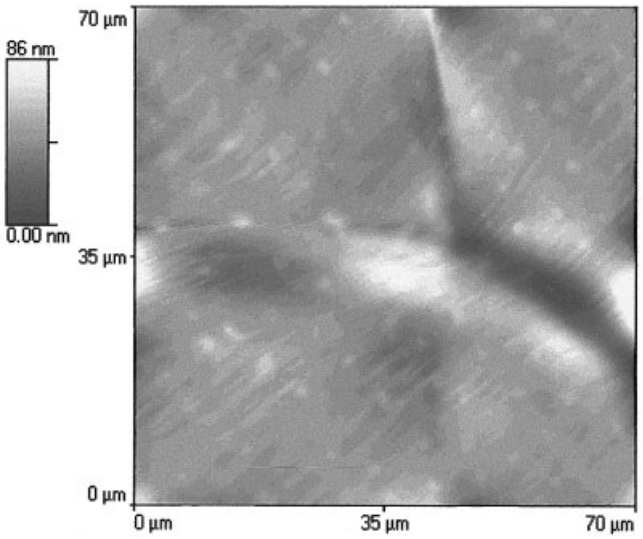

Figure 4 AFM image from a central area of the AP latex dry film. Depressions and neighboring elevations can be seen.

formity than the former, which is the opposite of what was observed by Wang et al.,[26] in another system, using poly(butyl methacrylate). According to these authors, films prepared with surfactant-free poly(butyl methacrylate) latex dispersions dry uniformly, and surfactant-containing latex films prepared with the same latex dry from the edges inward. A propagating front separates a transparent, dry region from a turbid, moist domain. In both instances, transparent and void-free films are produced. Comparing the results in ref. 26 with our data, we conclude that latex film drying patterns are strongly system-dependent.

RL1

In the earlier drying stages, the latex formed parallel stripes close to the glass substrate, with a width of approximately 70 μm (Fig. 6, top). Later, radial structures were formed, protruding out of the film surface, around a bright central circle (Fig. 6, center). The particles within the radial structures and the central ring resisted coalescence, even in the dry film, as shown in the bottom image of Figure 6.

Experiments were also performed with the other reconstituted latexes: RL2 (RL1 plus an anionic surfactant) and RL3 (DL plus a nonionic surfactant). The RL3 latex did not show any changes in the film drying pattern (not shown) in comparison with DL, but for RL2, a decrease was observed in the central area containing noncoalesced particles, seen as scattered light spots in Figure 7, in comparison with the RL1 film (Fig. 6, bottom).

DISCUSSION

The results presented in this article show that the surfactant, other dialyzable molecules, and ionic components of the latex serum have a major effect on the latex drying pattern and on the final film morphology. Otherwise, these results are in agreement with

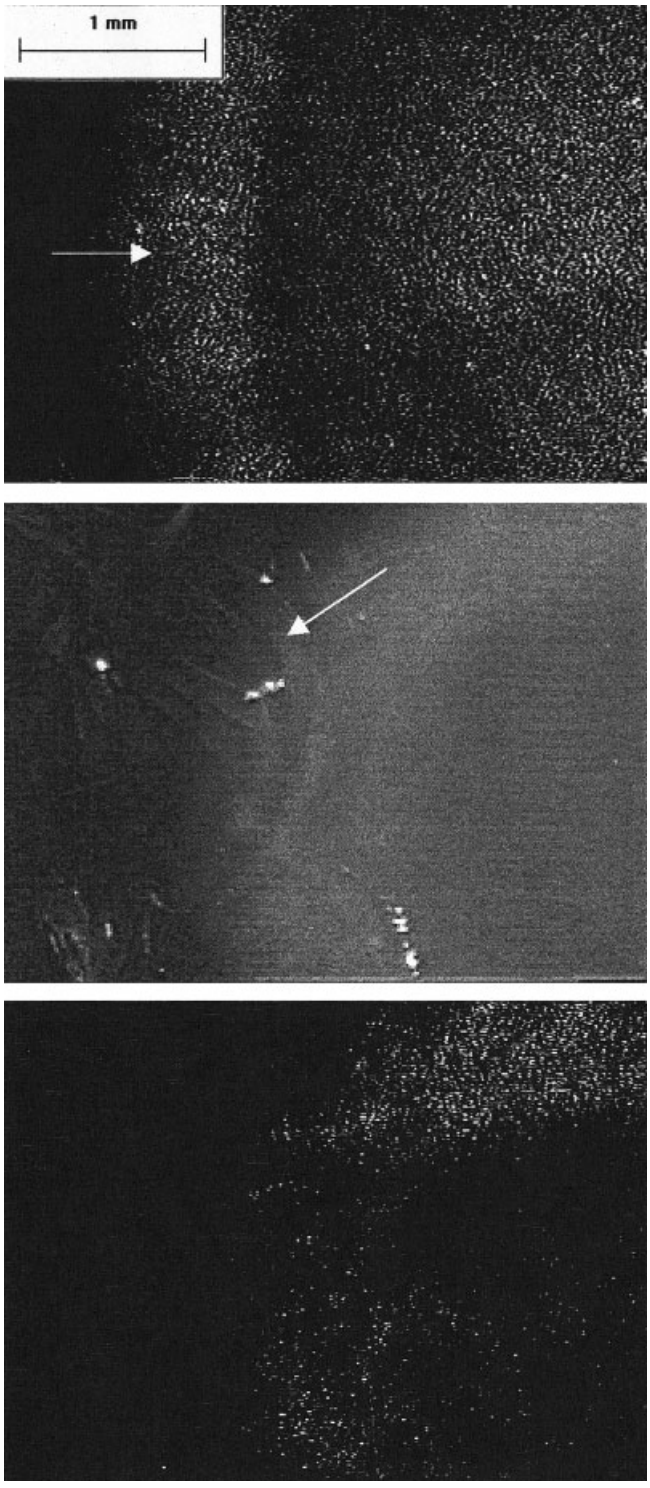

Figure 5 Images from DL latex film formation. The top image is an ultramicrograph showing an outer ring section, with large particle concentration fluctuations in contiguous domains. The center image, a reflected light view of stage 2, shows the surface film forming an almost circular structure (indicated by the arrow). Fast moving particles can be seen beneath it, but these are best observed by ultramicroscopy, as shown in the bottom image.

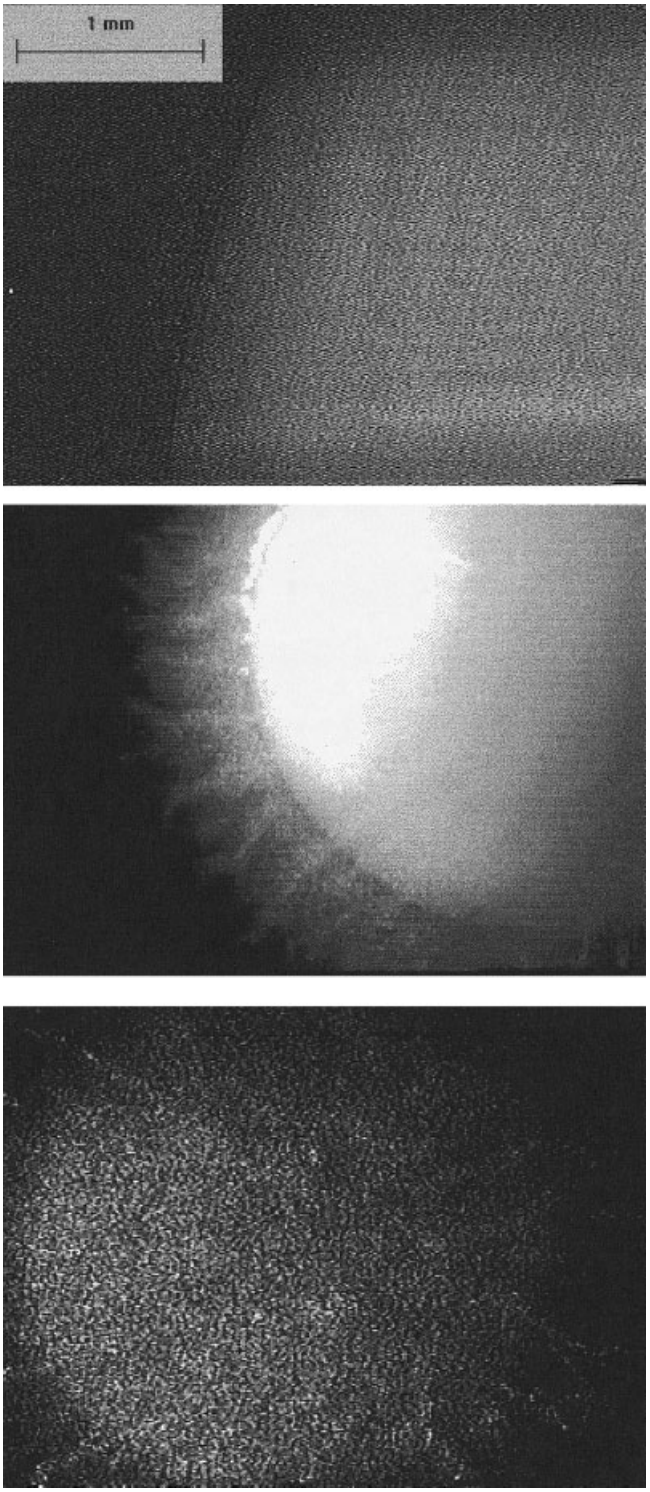

Figure 6 Images from RL1 latex film formation. The top image is an ultramicrograph showing roughly parallel stripes formed just above the substrate. The center image, a reflected light view taken at stage 2, shows radial structures. The bottom image, a dark-field image of the dry film in stage 3, shows uncoalesced particles.

Sheetz's[3] model for film formation, which means that the capillary forces deform a surface layer of particles, and the subsequent flow of water evaporating through this layer causes a compressive force on the particles beneath it, especially for the DL latex. These results suggest that we can make important gains in film quality by exercising careful control over trivial serum components.

Brownian individual particle motion is easily observed by ultramicroscopy, as used in this study, and its replacement by collective cluster motion is seen in the AP and DL latexes, as the rapid independent motion of bright dots is replaced by the slower concerted motion of neighboring bright dot arrays. This may be assigned to particle retardation by long-distance interactions due to the larger thickness of the diffuse double layers at low ionic strengths or to increased particle concentration. These results agree with those of Weeks et al.,[27] who observed cooperative PMMA particles motion as their volume fraction increased, and they reported this as a result of glasslike behavior in colloidal dispersions at volume fractions of 0.46–0.61.

The formation of a surface film trapping liquid beneath it is also observed in the dialyzed latex, contributing to the impairment of the overall dry film texture. This is probably a result of the absence of a surfactant monolayer on the drying film surface, together with the mutual electrostatic repulsion of the particles and the glass substrate. Okubo et al.[25] described skin formation at the surface of a latex dispersion, which was prevented by SDS addition, and they interpreted it as the result of flocculation due to particle–air interface instability. Tanimoto et al.[28] showed, using the evanescent wave technique, that at low salt concentrations the distance between PS particles and a glass substrate increased; in our case, this led to increased particle concentration at the liquid surface.

The formation of liquid latex domains with observable differences in the particle concentration is another factor responsible for the appearance of defects in the dry films. Many researchers have reported the formation of differentiated domains within a latex, under

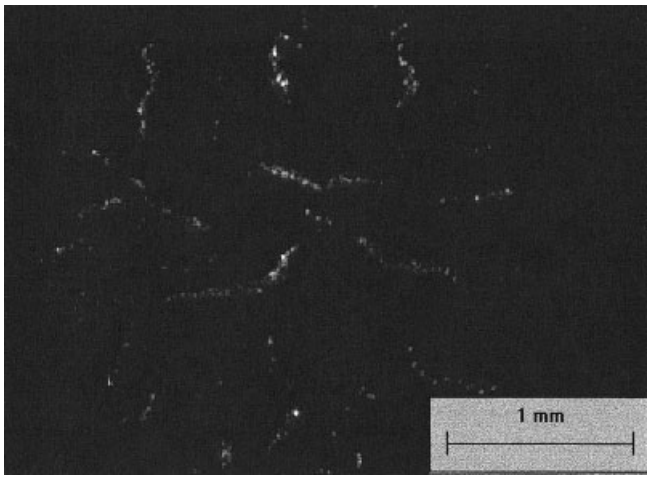

Figure 7 Dark-field image of the RL2 dry latex film. A comparison with the bottom image of Figure 6 shows the change in the distribution pattern on noncoalesced particles.

some special conditions. However, the correlation between latex domains and film defects has not been previously reported, to the best of our knowledge. For instance, Ito and coworkers[29,30] observed latex particle concentration fluctuations at low ionic strengths and low particle number densities, and they discussed their formation in detail. Joanicot et al.[10] observed the formation of ordered domains when a monodisperse, low ionic strength poly(styrene-*co*-butyl acrylate) dispersion dried over glass or quartz substrates, using small-angle neutron scattering. He and Donald[18] demonstrated by ESEM that ordered domains of core–shell PMMA–rubber–PMMA particles were disordered after salt addition and that fractal aggregates appeared during film drying. In this case, we assign the formation of defects in the central areas of AP and RL1 latex films to the accumulation of salt and surfactant in the final liquid pool, just before the completion of water evaporation.

Parallel stripes observed on the RL1 latex during stage 1 are probably a result of the interference of the laser beam due to the ordered array of the colloidal particles. Under different conditions (low ionic strength and low volume fraction), Yoshida et al.[22] demonstrated similar striplike patterns during an examination of PS latex particles by confocal microscopy.

The quality of film formation depends on the uniformity of the drying latex dispersion, which is, in turn, dependent on the formation of separated domains within the dispersion. Domains separate for two reasons. First, particle nonuniformity leads to particle clustering, which was recently demonstrated[31] and has now been confirmed in this work. Second, it may arise as a result of gas–liquid or gas–solid colloidal phase-separation phenomena,[32–34] which have been receiving greater attention in the literature.[35–37]

Colloidal phase separation has been assigned to the many-body attraction of particles of identical charge and the associated counterions,[38] thereby forming concentrated domains coexisting with domains of low particle concentration. Detailed calculations have shown that three particles carrying the same charge associate spontaneously and reversibly within some counterion concentration ranges.[39]

In summary, the large concentration gradients experimentally observed within the drying emulsion are probably important sources of the observed film heterogeneity, and this is consistent with the strong dependence of film quality on the serum composition.

CONCLUSIONS

Styrene/butyl acrylate latex film formation is strongly dependent on the latex serum components. Films obtained with the dialyzed latex are the most defective, whereas those made out of the as-prepared latex or with dialyzed latex after salt (but not surfactant) addition have the highest uniformity.

The addition of surfactants to the dialyzed latex does not improve film surface roughness, but it reduces the amount of noncoalesced particles in the film central region, as observed in the dialyzed latex to which salt was later added.

Large concentration fluctuations within the drying latex film are damaging to film quality, and its avoidance is needed if surface roughness is to be decreased. However, a more regular pattern of particle concentration in the substrate, such as that observed in the latex reconstituted by salt addition (RL1), leads to a uniform film. Large concentration fluctuations can be prevented by the avoidance of colloidal phase separation in the dispersion.

The presence of electrolytes and surfactants in the dispersion reduces skin formation during latex drying and also improves film surface quality.

F. Galembeck thanks Fapesp, Pronex/Finep, and CNPq for their continuing support. A. J. Keslarek is a Fapesp predoctoral fellow.

References

1. Dillon, W. E.; Matheson, D. A.; Bradford, E. B. J Colloid Sci 1951, 6, 108.
2. Brown, G. L. J Polym Sci 1956, 22, 423.
3. Sheetz, D. P. J Appl Polym Sci 1965, 9, 3759.
4. Vanderhoff, J. W.; Bradford, E. B.; Carrington, W. K. J Polym Sci Polym Symp 1973, 41, 155.
5. Winnik, M. A. Curr Opin Colloid Interface Sci 1997, 2, 192.
6. Keddie, J. L. Mater Sci Eng R 1997, 21, 101.
7. Visschers, M.; Laven, J.; German, A. L. Prog Org Coat 1997, 30, 39.
8. Steward, P. A.; Hearn, J.; Wilkinson, M. C. Adv Colloid Interface Sci 2000, 86, 195.
9. Klein, A. In Encyclopedia of Chemical Technology, 3rd ed.; Kirk, R. E.; Othmer, D. F.; Grayson, M.; Eckroth, D., Eds.; Wiley: New York, 1981; Vol. 14, p 82.
10. Joanicot, M.; Wong, K.; Marquet, J.; Chevalier, Y.; Pichot, C.; Graillat, C.; Lindner, P.; Rios, L.; Cabane, B. Prog Colloid Polym Sci 1990, 81, 175.
11. Morgans, W. M. Outlines of Paint Technology, 3rd ed.; Halsted: New York, 1990.
12. Routh, A. F.; Russel, W. B. Langmuir 1999, 15, 7762.
13. Feng, J.; Winnik, M. A. Macromolecules 1995, 28, 7671.
14. Keddie, J. L.; Meridth, P.; Jones, R. A. L.; Donald, A. M. Langmuir 1996, 12, 3793.
15. Dimonie, V. L.; El-Aasser, M. S.; Vanderhooff, J. W. Polym Mater Sci Eng 1980, 58, 821.
16. Adamson, A. W. Physical Chemistry of Surfaces, 5th ed.; Wiley: New York, 1990.
17. Dingenouts, N.; Ballauff, M. Langmuir 1999, 15, 3283.
18. He, C.; Donald, A. M. Langmuir 1996, 12, 6250.
19. Ito, K.; Muramoto, T.; Kitano, H. J Am Chem Soc 1995, 117, 5005.
20. Perrin, J. Les Atomes; Libraire Felix Alcan: Paris, 1913; Chapter 3.
21. Hunter, R. J. Foundations of Colloid Science; Oxford University Press: New York, 1991; Vol. 1.

22. Yoshida, H.; Yamanaka, J.; Koga, T.; Koga, T.; Ise, N.; Hashimoto, T. Langmuir 1999, 15, 2684.
23. Pike, E. R. In Scattering Techniques Applied to Supramolecular and Nonequilibrium Systems; Chen, S.-H.; Chu, B.; Nossal, R., Eds.; Plenum: New York, 1981.
24. Hwa, J. C. H. J Polym Sci Part A: Gen Pap 1964, 2, 785.
25. Okubo, M.; Takeya, T.; Tsutsumi, Y.; Kadooka, T.; Matsumoto, T. J Polym Sci Polym Chem Ed 1981, 19, 1.
26. Wang, Y.; Kats, A.; Juhué, D.; Winnik, M. A. Langmuir 1992, 8, 1435.
27. Weeks, E. C.; Crocker, J. C.; Levitt, A. C.; Schofield, A.; Weitz, D. A. Science 2000, 287, 627.
28. Tanimoto, S.; Matsuoka, H.; Yamaoka, H. Colloid Polym Sci 1995, 273, 1201.
29. Ito, K.; Nakamura, H.; Yoshida, H.; Ise, N. J Am Chem Soc 1988, 110, 6955.
30. Dosho, S.; Ise, N.; Ito, K.; Iwai, S.; Kitano, H.; Matsuoka, H.; Nakamura, I.; Okumura, H.; Ono, T.; Sogami, I. S.; Ueno, Y.; Yoshida, H.; Yoshiyama, T. Langmuir 1993, 9, 394.
31. Galembeck, F.; Braga, M.; Silva, M. C. V. M.; Herzog, A. Colloids Surf A 2000, 164, 217.
32. Hachisu, S.; Kobayashi, Y.; Kose, A. J Colloid Interface Sci 1973, 42, 342.
33. Kremer, K.; Robbins, M. O.; Grest, G. S. Phys Rev Lett 1986, 57, 2694.
34. Stevens, M. J.; Robbins, M. O. J Chem Phys 1993, 98, 2319.
35. Monovoukas, Y.; Gast, A. P. J Colloid Interface Sci 1989, 128, 533.
36. Sirota, E. B.; Ouyang, H. D.; Sinha, S. K. Phys Rev Lett 1989, 62, 1524.
37. Crocker, J. C.; Grier, D. G. MRS Bull 1998, 23, 24.
38. Chan, D. Y. C.; Linse, P.; Petris, S. N. Langmuir 2001, 17, 4202.
39. Wu, J. Z.; Bratko, D.; Blanch, H. W.; Prausnitz, J. M. Phys Rev 2000, 62, 5273.